The thermal decomposition kinetics of carbonaceous and ferruginous manganese ores in atmospheric conditions

by S.A.C. Hockaday[1,2], F. Dinter[2], and Q.G. Reynolds[3,4]

Affiliation:
[1]Western Australia School of Mines, Curtin University, Australia.
[2]Department of Mechanical and Mechatronic Engineering, University, Stellenbosch, South Africa.
[3]Department of Process Engineering, Stellenbosch University, South Africa.
[4] Extractive Metallurgy Division, Mintek, South Africa.

Correspondence to:
L. Hockaday

Email:
lina.hockaday@curtin.edu.au

Dates:
Received: 14 Dec. 2022
Revised: 3 Jul. 2023
Accepted: 10 Aug. 2023
Published: August 2023

How to cite:
Hockaday, S.A.C., Dinter, F., and Reynolds, Q.G. 2023
The thermal decomposition kinetics of carbonaceous and ferruginous manganese ores in atmospheric conditions.
Journal of the Southern African Institute of Mining and Metallurgy, vol. 123, no. 8. pp. 391–398

DOI ID:
http://dx.doi.org/10.17159/2411-9717/2527/2023

ORCID:
L. Hockaday
https://orcid.org/0000-0003-2597-9756

Synopsis

The thermal decomposition of carbonate minerals as pre-treatment before smelting reduces the energy requirement for smelting. It can also make the combustion of fossil fuels for heating unnecessary. Thermal decomposition may become important in reducing greenhouse gas emissions when producing ferromanganese alloys while simultaneously reducing electrical energy demand during smelting. A kinetic reaction rate model for the thermal decomposition of manganese ores is presented, based on published reaction rate kinetics for the decomposition of manganese oxides and calcium carbonate. The model was validated against thermogravimetric data for two carbonaceous manganese ore samples and one ferruginous manganese ore sample. The reaction rate model shows that carbonate minerals in the manganese ores are decomposed at temperatures above 900 °C while pyrolusite is decomposed at temperatures from 450 °C to 500 °C. Mn_2O_3 decomposes rapidly at 550 °C. Braunite decomposition at temperatures below 1000 °C was negligible. The presence of organic carbon in the samples led to further reduction of the samples during thermal treatment.

Keywords

manganese ore, pre-treatment, thermal decomposition, reaction rate modelling.

Introduction

Manganese ores have complex mineralogy (Chetty, 2008). Although most South African manganese ores manganese oxides such as pyrolusite, bixbyite, braunite and hausmannite, they are often associated with gangue minerals such as calcite, kutnahorite, ankerite and dolomite. These carbonate minerals undergo endothermic decomposition reactions that increase the energy demand for ferromanganese alloy production. In contrast, the higher manganese oxides undergo mainly exothermic reduction reactions with solid carbon and carbon monoxide, which are desirable in smelting as they reduce the overall energy demand of the process. Pre-treatment methods for manganese ores may be categorized as pre-heating, calcination, or agglomeration.

Pre-heating has been practised to reduce the electricity demand of ferromanganese submerged arc furnaces (Tanabe, 1968; Ishak and Tangstad, 2007; Tangstad, Ichihara and Ringdalen, 2015) by using combustion of fossil fuels or furnace off-gas to pre-heat the feed. This practice has inspired more research into the pre-heating and pre-reduction of manganese ores not just with furnace off-gas, but also with bio-carbon and indirect use of solar thermal energy (Hockaday *et al.*, 2020; Mckechnie, McGregor and Venter, 2020; Hamuyuni *et al.*, 2021; Julia *et al.*, 2021; Kazdal *et al.*, 2021).

Calcination is generally not practised as feed preparation for ferroalloy production due to the requirements for strong lumpy ore as the solid burden in a submerged arc furnace. The solid burden in the furnace acts similarly to that in a vertical kiln; it is heated and reduced by carbon monoxide evolved from the reduction of MnO to metallic manganese in the coke bed (Olsen, Tangstad and Lindstad, 2007). However, the advantages of such preheating have been evaluated and it was found that preheating carbonate-rich manganese ores may reduce the electric energy demand for ferroalloy production by 25% for cooled thermally treated ore and by 35 % for hot charged thermally treated ore (Serov, 2007).

Currently, sintering is the leading pre-treatment technology for manganese ores. Sintering is used to agglomerate fines (<6 mm) into furnace feed. Although not traditionally seen as a reducing process, sintering is done in reducing conditions with solid carbon as the reductant at temperatures of 1200°C or above (Pienaar and Smith, 1992; Daavittila *et al.*, 2001). Although sintering decomposes carbonate minerals, it also reduces the manganese oxides to hausmannite and manganosite leading to a trade-off where sintered

products require less energy for carbonate decomposition during smelting but lose the benefit of energy from exothermic manganese reduction reactions (Broekman and Ford, 2004) under smelting conditions. The use of physical separation techniques such as dense media separation or flotation to upgrade manganese ores by removing gangue minerals such as silica or calcite has not been widely applied as the success of these methods is dependent on the mineralogy of the ores. Ore samples evaluated for this paper show finely intergrown structures even on the 20 µm scale (Hockaday *et al*., 2021), making upgrading by physical separation methods impractical due to the fine particle size required to fully liberate the gangue minerals. The successful use of dense medium separation has been described (Pienaar and Smith, 1992) for Mamatwan ore, but the results may not be replicable on other ores with finely intergrown minerals. The evaluation of physical separation as an alternative or complementary beneficiation method for manganese ores is outside the scope of this paper.

The question then arises if it is possible to decompose the carbonate minerals while preventing or hindering the reduction of the oxide minerals? Less reliance on the use of fossil fuels for heating, lowering of the energy demand for smelting and avoidance of the Boudouard reaction during smelting to avoid increased reductant demand are three reasons for a thermal pre-treatment step in oxidative conditions. We developed a reaction rate model describing the behaviour of the ores for thermal treatment under atmospheric conditions. The model will be useful in further investigations of manganese ore pre-treatment in oxidizing conditions using renewable energy sources such as electricity from renewables or direct concentrating solar thermal treatment to achieve the required temperatures. This makes developing a non-reducing thermal pre-treatment for manganese ores a promising route for greener ferromanganese production.

Theory

Thermal pre-treatment has been recommended for carbonaceous manganese ores (Serov, 2007) in Russia using furnace off-gas for pre-heating and pre-reduction. The thermal decomposition reactions for the carbonate minerals are:

$$CaMg(CO_3)_2 \rightarrow CaO + MgO + 2CO_2(g), \quad \Delta H_1 = +302\ \text{kJ}; \quad [1]$$

$$CaCO_3 \rightarrow CaO + CO_2(g), \quad \Delta H_2 = +178\ \text{kJ}; \quad [2]$$

$$MgCO_3 \rightarrow MgO + CO_2(g), \quad \Delta H_3 = +101\ \text{kJ}. \quad [3]$$

Since the composition of kutnahorite, $Ca(Mn, Mg)(CO_3)_2$, is stoichiometrically variable, the decomposition of kutnahorite was modelled as a combination of Equations [1], [2], and [3]. This enables the modelling of ores with high variability in mineralogy.

These reactions are endothermic as seen from the positive enthalpy of the reaction, ΔH. Enthalpy values were obtained from the HSC Reaction module (Roine and Bjorklund, 2002; Outotec, 2019) at standard conditions of 25°C and 1 atmosphere. Avoiding these reactions inside the smelter reduces the energy demand for smelting, increasing the smelter's productivity. If these carbonate minerals decompose inside the smelter, the released carbon dioxide may react with solid carbon according to the Boudouard Equation [4]:

$$1 - (1 - X_i)^{\frac{1}{2}} = k_i t, \quad [4]$$

This leads to increased reductant consumption inside the furnace and higher energy demand to maintain smelting temperatures. Although most South African ores have lower concentrations of carbonate minerals than the Russian ores, the benefits of decomposing the carbonates before smelting are clear, especially for the ores containing dolomite.

The thermal decomposition of $CaCO_3$ has been studied (Hills, 1968; Ar and Doğu, 2001; Halikia *et al*., 2001) due to its importance in cement production. The rate-limiting step has been determined as either the chemical reaction at the interface (Ar and Doğu, 2001; Halikia *et al*., 2001) or heat and mass transfer (Hills, 1968). The decomposition rate of different $CaCO_3$ sources may vary significantly (Ar and Doğu, 2001), so it is important to validate the kinetic rate expression against measured data. For this study, the calcination reactions are assumed to be limited by the contracting area mechanism (Halikia *et al*., 2001), with the integrated rate equation expressed as

$$1 - (1 - X_i)^{\frac{1}{2}} = k_i t, \quad [5]$$

where X_i is the conversion extent of reaction i, t is the time, and k_i is the reaction rate frequency factor, dependent on temperature according to the Arrhenius equation,

$$k_i = A_i e^{\frac{-E_{ai}}{RT}} \quad [6]$$

with A_i the pre-exponential factor, E_{ai} the activation energy, T the temperature in Kelvin and R the universal gas constant.

Manganese oxides can also decompose thermally in air. The reactions are as follows

$$4MnO_2 \rightarrow 2Mn_2O_3 + O_2(g), \quad \Delta H_5 = +162\ \text{kJ}; \quad [7]$$

$$6Mn_2O_3 \rightarrow 4Mn_3O_4 + O_2(g), \quad \Delta H_6 = +220\ \text{kJ}; \quad [8]$$

$$3Mn_7SiO_{12} \rightarrow 7Mn_3O_4 + 3SiO_2 + O_2(g), \quad \Delta H_7 = +364\ \text{kJ}. \quad [9]$$

The reaction kinetics of reaction Equations [7] and [8] has been studied (Terayama and Ikeda, 1983) and found to be limited by interfacial chemical reaction. Further studies on reaction kinetics for reaction Equation [8] were done to investigate using manganese oxides as a redox pair for water splitting (Botas *et al*., 2012; Alonso, Gallo and Galleguillos, 2016) and the contracting volume mechanism was found to describe the data well, although the n^{th} order mechanism was found to improve the model fit.

The thermal decomposition of Mn_7SiO_{12}, Equation [9], has been reported (Grimsley, See and King, 1977) as occurring above 900°C, but no published studies were found on the kinetics of this reaction. For this study, the manganese oxide decomposition reactions will be assumed to be limited by the contracting volume mechanism (Terayama and Ikeda, 1983), with the integrated rate equation expressed as

$$1 - (1 - X_i)^{\frac{1}{3}} = k_i t. \quad [10]$$

Manganese ores may contain some hydrated minerals, and the mass loss at temperatures below 300°C is expected to be from the evaporation of surface water or the dewatering of hydrated minerals.

The manganese ore samples was found to contained significant amounts of organic carbon, up to 3% by weight. The organic carbon source is unknown but may be from the untreated ore (plant or bio-matter) or from contamination at the smelter site (from reductant).

The organic carbon content was modelled as pure graphite in this study.

The kinetics of the direct reduction of manganese ore pellets containing carbon has been studied (Zhang and Xue, 2013), and a kinetic model in two stages was proposed. The earlier stage proceeds with carbon as a reducing agent and the kinetic expression for a contracting volume as applied to the non-isothermal method according to Equation [10]. This reaction rate was applied to the possible reduction reactions simultaneously. The later stage regarding reduction reactions with carbon monoxide was neglected as the sample mass loss was fully explained by reduction with solid carbon. The reactions with solid carbon considered in this study are:

$$2MnO_2 + C \rightarrow Mn_2O_3 + CO(g);\ \Delta H_{12} = -29\ kJ; \quad [11]$$

$$3Mn_2O_3 + C \rightarrow 2Mn_3O_4 + CO(g);\ \Delta H_{13} = -0.3\ kJ; \quad [12]$$

$$Mn_3O_4 + C \rightarrow 3MnO + CO(g);\ \Delta H_{14} = +117\ kJ \quad [13]$$

$$\frac{3}{2}Mn_7SiO_{12} + C \rightarrow \frac{7}{2}Mn_3O_4 + \frac{3}{2}SiO_2 + CO(g);\ \ \Delta H_{15} = +71\ kJ; \quad [14]$$

$$3Fe_2O_3 + C \rightarrow 2Fe_3O_4 + CO(g);\ \Delta H_{16} = +133\ kJ; \quad [15]$$

$$Fe_3O_4 + C \rightarrow 3FeO + CO(g);\ \Delta H_{17} = +210\ kJ; \quad [16]$$

$$FeO + C \rightarrow Fe + CO(g);\ \Delta H_{18} = +155\ kJ. \quad [17]$$

Experimental methodology

The ore samples obtained from the Transalloys ferromanganese smelter in South Africa were characterized by chemical analysis and mineralogical method. The fines were screened from the fresh ore – these are usually briquetted with dust and metal fines before smelting (Steenkamp *et al.*, 2018). Chemical analysis was done by inductively coupled plasma discharge optical emission spectroscopy (ICP-OES). The carbonate content was determined from the difference between total carbon and organic carbon by combustion analysis. The mineralogy of the ores was investigated by X-ray diffraction analysis and scanning electron microscopy. More details on the sample mineralogy are reported elsewhere (Hockaday, 2023, Chapter 3) as the focus of this paper was on the reaction kinetics modelling. Cryptomelane (KMn_8O_{16}) was expressed in manganese oxide form as

$$KMn_8O_{16} \rightarrow \frac{1}{2}K_2O + 7MnO_2 + \frac{1}{2}Mn_2O_3 \quad [18]$$

to simplify the decomposition of the ore while maintaining the oxidation state of manganese.

After reconciling the chemical analysis and mineralogical data, the compositions of the ore samples are reported in Table I.

These compositions took into account the thermal behaviour of the samples as well, as the high-cryptomelane ore (CMN) showed faster carbonate decomposition than the high braunite ore (BMN), which was captured by expressing Mg content as $MgCO_3$ rather than $CaMg(CO_3)_2$. Since the tests were done in triplicate and this behaviour was consistent for the ore in all three tests, it was included in the model. This does not imply that the mineralogical analysis was in error, but rather that decomposition of the carbonate minerals occurred differently in the two ores investigated. This is

Table I

Composition of three manganese ore samples (wt.%)

	Ferruginous Mn ore (FMN)	High-braunite Mn ore (BMN)	High-cryptomelane Mn ore (CMN)
MnO_2	17.81	2.56	17.08
$Mn7SiO_{12}$	14.78	41.74	27.02
Mn_2O_3	0.83	0.84	1.85
Mn_3O_4	–	7.19	7.87
SiO_2	13.58	3.42	6.21
Fe_2O_3	31.94	6.18	6.87
K_2O	1.62	0.05	1.10
Cr_2O_3	0.08	0.51	–
P_2OY_5	0.09	0.06	0.07
$BaSO_4$	0.40	0.37	0.30
Na_2O	0.55	0.03	0.21
Organic carbon, C	3.44	1.78	1.92
$CaMg(CO_3)_2$	–	17.61	-
$CaCO_3$	–	16.48	20.00
CaO	1.76	–	1.68
MgO	0.66	–	–
$Mn_2O_3.3H_2O$	1.89	0.09	0.72
Al_2O_3	10.57	–	–
$Al_2O_3.3H_2O$	–	1.09	0.98
$MgCO_3$	–	–	6.12

most likely due to mineralogical differences outside of the scope of the current study, and which indicate that more in-depth research is required into the mechanisms of thermal decomposition as related to carbonate gangue minerals in manganese ores. For now, this study concluded that thermogravimetric studies should be included in the characterization of ores where different carbonate minerals are present and the thermal decomposition behaviour needs to be accurately modelled even at lower temperatures (300–800°C).

Experimental set-up

The non-isothermal tests were done at Mintek's high-temperature test facilities in Randburg, South Africa. The tests were done using an electrically heated tube furnace with a recrystallized alumina tube of 50 mm internal diameter. A Eurotherm thyristor-coupled controller, connected to a B-type thermocouple suspended just above the sample, controlled the furnace temperature. The sample was placed in an alumina crucible and raised into the furnace on an alumina pedestal and rod resting on a digital electronic balance. The balance and sample were moved with a hydraulic hoisting mechanism.

Weight loss was recorded on a personal computer interfaced with the balance. Milled samples were treated in the furnace at a ramp rate of 4°C per minute up to 1000 °C in air. The calcined products were not tested, as the study looked at the mass loss of the sample as representative of the changes in the minerals. However, other studies looking at the behaviour of these ores when heated directly with concentrating solar radiation or in a muffle furnace report analyses of the products (Hockaday *et al.*, 2018, 2019, 2021; Hockaday, 2023).

Reaction rate model methodology

Three samples from each ore were treated in the thermogravimetric furnace, and the recorded mass loss curves were used to inform the reaction rate model describing the thermal behaviour. The rate equations were fitted to one of the three sets of experimental data. Figure 1 shows the measured sample mass of a ferruginous Mn ore (FMN) sample and the predicted sample mass from a model based on published reaction rate parameters and the model with parameters fitted to the measured data. Since the ferruginous sample did not contain carbonate minerals, the reactions evaluated were the thermal decomposition of MnO_2 to Mn_2O_3 and Mn_2O_3 to Mn_3O_4 and the reduction reactions with solid carbon (Equations [11] – [17]).

The resulting reaction rate equations were then used in an HSC simulation with the measured temperature profiles of the remaining two tests for the ore sample as input to estimate the samples' mass loss as output for one-minute intervals. The plots of the modelled sample mass against the measured sample mass validated the model for that specific ore. Figure 2 shows the validation for the ferruginous ore model with the modelled sample mass within 2% of the measured sample mass for both validation tests.

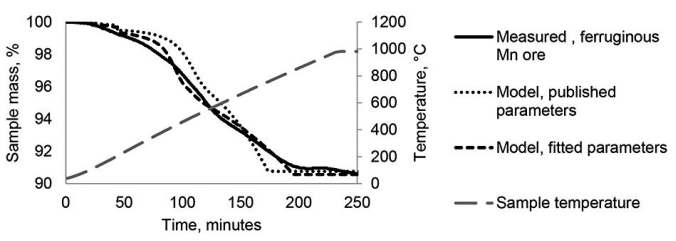

Figure 1—Ferruginous ore measured and modelled mass loss with measured temperature

The parameters fitted with the ferruginous ore were transferred to the high braunite and high-cryptomelane ores models. The measured sample mass of the high-braunite ore was used to fit parameters for the thermal decomposition of dolomite and calcite (Equations [1] and [2]). The measured values and modelled values are shown in Figure 3.

The validation for the high braunite Mn ore (BMN) is shown in Figure 4. The BMN model reflects the slower decomposition of $CaCO_3$ in the high braunite ore with an activation energy of 190 kJ/mol compared to the published value of 155 kJ/mol (Halikia *et al.*, 2001). The modelled values are within 4 % of the measured values for the first validation test and within 2% of the measured values for the second test.

The mass loss for the high-cryptomelane ore was used to estimate the thermal decomposition of $MgCO_3$ and confirm the calcite decomposition rate. The measured and modelled sample mass values are shown in Figure 5.

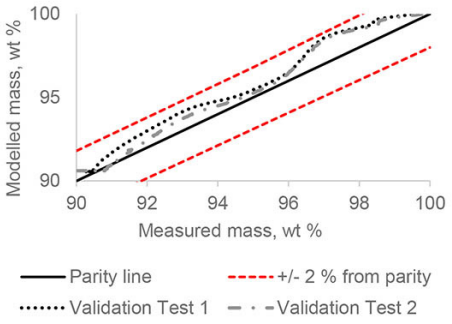

Figure 2—Model validation for ferruginous ore reaction rates by comparison of modelled and measured sample mass values

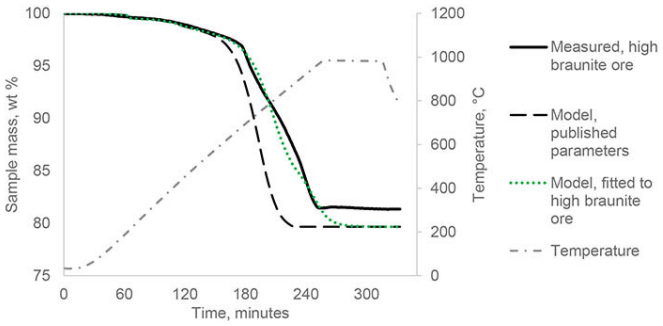

Figure 3—High braunite ore measured and modelled sample mass with measured temperature profile

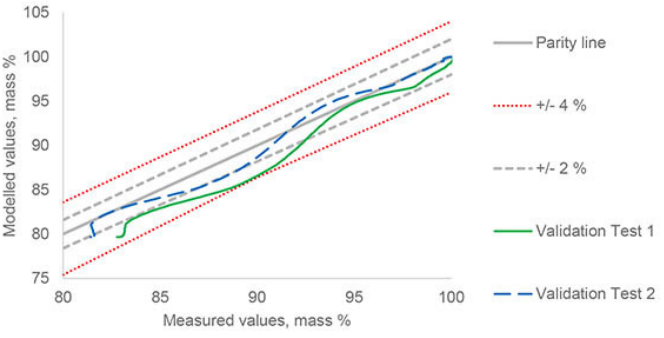

Figure 4—Model validation for high braunite ore reaction rates by comparison of modelled and measured mass loss values

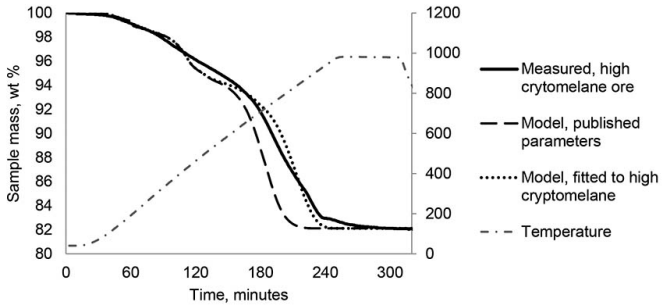

Figure 5—High cryptomelane ore measured and modelled sample mass with measured temperature profile

The validation results for the high-cryptomelane ore (CMN) are shown in Figure 6. The modelled sample mass remained within 2% of the measured sample mass. The CMN model showed faster decomposition of $CaCO_3$ than the high braunite ore with an activation energy of 175 kJ/mol. The difference in calcite decomposition rates for different ore samples is not unexpected, as even high-purity calcites have been shown to vary greatly in decomposition behaviour (Ar and Doğu, 2001).

The kinetic rate equations, activation energies, and pre-exponential factors determined from the experiments are summarized in Table II.

Results and discussion

The developed models were used to estimate the sample composition during heating. The normalized content of manganese compounds and organic carbon (modelled as pure graphite, C) during the thermal treatment (at a heating rate of 4°C/min up to 1000°C) is shown for the ferruginous Mn ore in Figure 7. For clarity, the reduction of iron oxides has not been shown, but iron oxides were reduced simultaneously with the manganese oxides while carbon was present in the system to a final mixture of Fe_3O_4 (18.8 wt.%) and FeO (8.2 wt.%) with some Fe_2O_3 (3.5 wt.%) and Fe (2.2 wt.%).

The decomposition and reduction of MnO_2 and Mn_2O_3 were complete by 500°C and 550°C, respectively. Reduction of Mn_3O_4 and Mn_7SiO_{12} continued while solid carbon was present in the system. Similarly, the normalized compositions of manganese compounds, carbonate minerals, and organic carbon during thermal treatment for the high-braunite ore are shown in Figure 8.

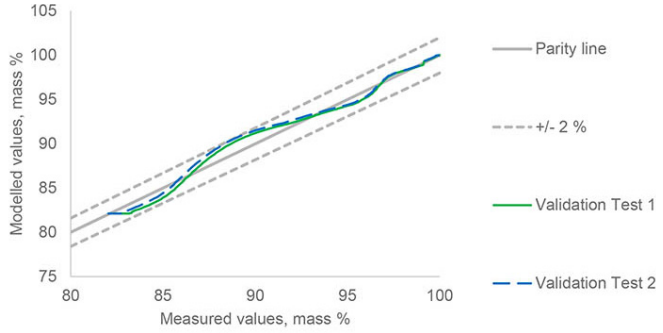

Figure 6—Model validation for high cryptomelane ore reaction rates by comparison of modelled and measured mass loss values

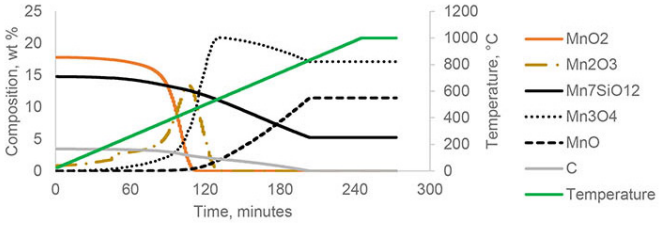

Figure 7—Modelled ferruginous manganese ore compositional changes during thermal treatment

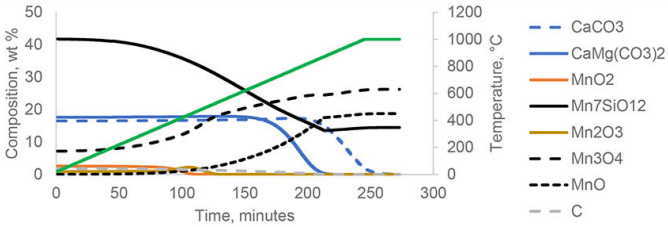

Figure 8—Modelled high-braunite ore compositional changes during thermal treatment

Since the braunite ore has a very low content of MnO_2 and Mn_2O_3, mass loss can be attributed mainly to the reduction of braunite (Mn_7SiO_{12}) and the thermal decomposition of carbonate minerals modelled as dolomite ($CaMg(CO_3)_2$) and calcite ($CaCO_3$). Calcite decomposition only started at around 850 °C, indicating that calcination temperatures of at least 900°C are required to achieve full calcination of this ore.

Table II

Reaction rate equations, activation energies and pre-exponential factors determined from experimental data

Reaction	Rate equation	Reference proposing rate equation	E_{ai} kJ/mol	A_i
[1] [2]	$1-(1-X_i)^{\frac{1}{2}}$	– Halikia *et al.* (2001)	165 190 (BMN) 175 (CMN)	4 368 805 4 368 805
[3]	0.6% for 100 °C < T < 400 °C $1-(1-X_i)^{\frac{1}{2}}$ for T > 400 °C	– –	– 165 (CMN)	4 368 805
[7] [8]	$1-(1-X_i)^{\frac{1}{3}}$	Terayama and Ikeda (1983)	62.6 65.5	23 426 100 4 072 865
[11] to [17]	$1-(1-X_i)^{\frac{1}{3}}$	Zhang and Xue, (2013)	18.0	0.00038

The normalized compositions of manganese compounds, carbonate minerals, and organic carbon during thermal treatment for the high cryptomelane ore are shown in Figure 9.

The cryptomelane ore has a higher content of oxidized manganese compounds and, similar to the ferruginous ore, the decomposition and reduction of MnO_2 and Mn_2O_3 were complete by 500°C and 550°C respectively. The decomposition of calcite in this ore started at around 720 °C, and full calcination was reached at 950°C. The reduction of braunite and Mn_2O_3 continued while solid carbon was available in the system resulting in 11.6 wt% of MnO in the treated sample.

From the results, the thermal decomposition of MnO_2 and Mn_2O_3 will always be completed before the calcination of the ores, and cannot be limited by choice of operational temperature without impacting the degree of calcination. The reduction of all manganese oxides will start even at 350°C but may be limited by the amount of solid carbon available. This is illustrated for the two carbonate-rich ores in Figures 10 and 11, where scenarios without organic carbon in the ore are compared to the ores as received. It may also be seen that this strategy would be more effective for the high-braunite ore, as braunite did not thermally decompose over the temperature range investigated.

The calculated composition of the three ores after thermal pre-treatment is given in Table III.

Significant amounts of braunite (Mn_7SiO_{12}) and hausmannite (Mn_3O_4) remain after the thermal treatment. These compounds will react with carbon monoxide during smelting according to the following reactions,

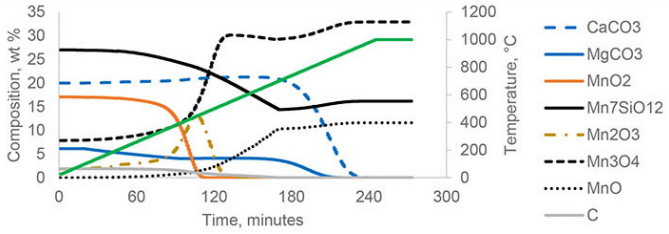

Figure 9— Modelled cryptomelane ore compositional changes during thermal treatment

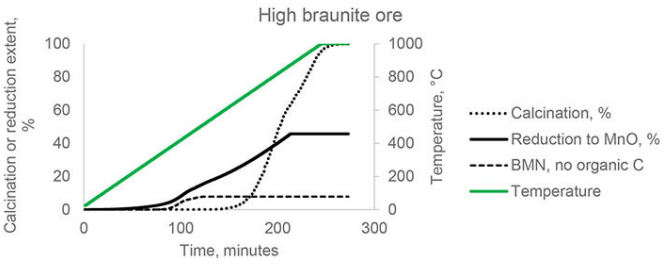

Figure 10—Modelled calcination and reduction of manganese oxides for high-braunite ore

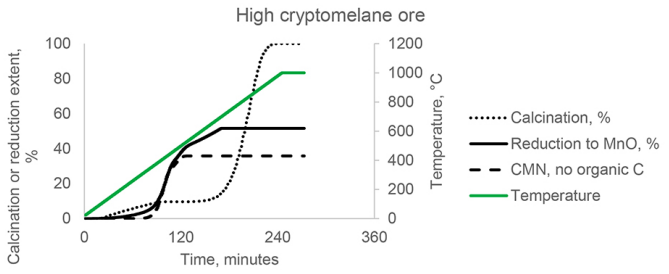

Figure 11—Modelled calcination and reduction of manganese oxides for high-cryptomelane ore

Table III

Modelled composition of thermally treated ores based on composition in Table I

	Modelled thermally treated composition		
	FMN	BMN	CMN
Mn_7SiO_{12}	5.18	14.27	16.26
Mn_3O_4	17.08	26.44	32.58
SiO_2	16.10	8.08	9.22
Fe_2O_3	3.51	0.57	1.99
K_2O	1.79	0.06	1.34
Cr_2O_3	0.09	0.64	–
P_2O_5	0.10	0.08	0.09
$BaSO_4$	0.44	0.46	0.37
Na_2O	0.61	0.04	0.26
CaO	1.94	18.31	15.69
MnO	11.53	18.76	11.87
Fe_3O_4	18.79	3.93	4.66
MgO	0.73	4.83	3.56
FeO	8.21	1.99	1.17
Fe	2.24	0.64	0.18
Al_2O_3	11.67	0.89	0.78

$$Mn_3O_4 + CO(g) \rightarrow 3MnO + CO_2(g),\ \Delta H_{19} = -55\ \text{kJ}; \quad [19]$$

$$3Mn_7SiO_{12} + 2CO(g) \rightarrow 7Mn_3O_4 + 3SiO_2 + 2CO_2(g),\ \Delta H_{20} = -202\ \text{kJ}. \quad [20]$$

These exothermic reactions will result in reduced energy demand during smelting compared to manganese sinter, which has been fully reduced to MnO.

The thermally pre-treated material can be introduced as feed to briquetting plants or agglomerated with low-temperature binders (Devasahayam, 2018) to achieve the strength requirements of blast furnaces or submerged arc furnaces during high-carbon ferromanganese production.

The specific energy requirement (SER) to produce a high-carbon ferromanganese alloy (78% Mn, 7.5%C, remainder Fe) at 1300°C, slag at 1500°C, and off-gas at 700°C, was estimated based on an HSC distribution model with carbon addition of twice the stoichiometric requirement and assumptions based on published literature (Broekman and Ford, 2004). For untreated high-braunite ore, the SER was calculated as 2.31 MW/t alloy produced. After oxidative thermal treatment, the SER was calculated as 0.98 MW/t alloy produced. This is a reduction of electricity demand of more than 50%. Since the South African national grid is supplied by mainly coal fired power plants, the reduction in scope 2 emissions is similarly significant. Compared to a sinter produced from this material (assuming MnO/Mn_2O_3 mass ratio in the sinter of 0.42 (Daavittila *et al.*, 2001)), the sinter SER was calculated as 1.21 MW/t alloy. For this ore, thermal pre-treatment results in a product with an SER lower than that for sinter, with 0.36 t carbon dioxide emissions less per ton of product.

For untreated high-cryptomelane ore, the calculated SER was 1.66 MW/t alloy produced. After oxidative thermal treatment, the calculated SER was 1.00 MW/t alloy produced. This is a reduction of almost 40 % in electricity demand. Comparing to a sinter produced from this material (assuming a MnO/Mn_2O_3 mass ratio in the sinter of 0.42 (Daavittila *et al*., 2001)), the sinter SER was calculated as 0.77 MW/t alloy. Thermal decomposition for this ore results in a product with an SER higher than sinter. Sinter production will however result in additional 0.36 t CO_2 emissions per ton of ore treated due to fuel combustion.

Conclusion

A reaction rate model describing the behaviour of three different manganese ores was developed based on published kinetic rate equations. The model uses a system of rate equations to describe the thermal decomposition and reduction with solid carbon of the ores and was validated to predict sample mass values within 2% to 4% of the measured values.

The reaction rate model indicates that the thermal decomposition of carbonate minerals occurs quickly above 900°C and does not start before 720°C. The calcite decomposition kinetics differ for the carbonate ores, with the high-cryptomelane ore showing calcite decomposition at lower temperatures than the high braunite ore.

Thermal decomposition of MnO_2 occurs first and is completed at 500°C. The thermal decomposition of Mn_2O_3 follows and is complete at 550°C. The thermal decomposition of Mn_3O_4 and Mn_7SiO_{12} was found to not occur below 1000°C, but the reduction of Mn_3O_4 and Mn_7SiO_{12} with solid carbon occurs while solid carbon remains available.

The study of the kinetics of the thermal decomposition of manganese ores containing carbonates indicates that thermal pre-treatment in oxidative conditions can decompose carbonate minerals while maintaining a high degree of manganese oxidation if no solid carbon is present. MnO_2 and Mn_2O_3 thermally decompose without any reductant, but Mn_3O_4 and Mn_7SiO_{12} are stable in the absence of a reductant at temperatures below 1000°C.

The thermal treatment of high-braunite, high-carbonate manganese ores decompose carbonate minerals without additional scope 2 greenhouse gas emissions. This leads to a lower electricity demand for ferromanganese production in submerged arc furnaces of up to 50 %. Weight reduction of 15 to 20% during thermal treatment results in significantly lower transport costs as well.

Acknowledgements

This paper is published by permission of Mintek. The authors would like to acknowledge Transalloys for providing the ore samples studied.

Credit author statement

SACH: Conceptualization, Methodology, Validation, Visualisation, Original draft preparation, Funding

FD, QR: Supervision, Review.

References

Alonso, E., Gallo, A., and Galleguillos, H. 2016. Solar Thermal Energy Use in Lead-Acid Batteries Recycling Industry: A Preliminary Assessment of the Potential in Spain and Chile. *Proceedings of EuroSun2016*. EuroSun2016, Palma de Mallorca, Spain: International Solar Energy Society. pp. 1–10. doi.org/10.18086/eurosun.2016.02.17

Ar, İ. and Doğu, G. 2001. Calcination kinetics of high purity limestones. *Chemical Engineering Journal,* vol. 83, no. 2. pp. 131–137. doi.org/10.1016/S1385-8947(00)00258-8

Botas, J.A., Marugan, J., Molina, R., and Herradon, C. 2012. Kinetic modelling of the first step of Mn2O3/MnO thermochemical cycle for solar hydrogen production. *International Journal of Hydrogen Energy*, vol. 37, no. 24. pp. 18661–18671. doi.org/10.1016/j.ijhydene.2012.09.114

Broekman, B.R. and Ford, K.J.R. 2004. The Development and Application of a HCFeMn Furnace Simulation Model for Assmang Ltd. *Proceedings Tenth International Ferroalloys Congress. INFACON X: 'Transformation through Technology'*, Cape Town, South Africa. Southern African Institute of Mining and Metallurgy. pp. 194–205.

Chetty, D. 2008. A geometallurgical evaluation of the ores of the northern Kalahari manganese deposit. South Africa (PhD thesis). University of Johannesburg.

Daavittila, J., Krogerus, H., Oikarinen, P., and Sarkkinen, R. 2001. Sintered Manganese Ore and Its Use in Ferromanganese Production. *Proceedings of the Ninth International Ferroalloy Congress. INFACON IX,* Quebec City, Canada. pp. 212–222. https://www.pyrometallurgy.co.za/InfaconIX/212-Jorma.pdf

Devasahayam, S. 2018. A novel iron ore pelletization for increased strength under ambient conditions. *Sustainable Materials and Technologies*, vol. 17. p. e00069. doi.org/10.1016/j.susmat.2018.e00069

Grimsley, W.D., See, J.B., and King, R.P. 1977. The mechanism and rate of reduction of Mamatwan manganese ore fines by carbon'. *Journal of The South African Institute of Mining and Metallurgy*. pp. 51–62

Halikia, I., Zoumpoulakis, L., Christodoulou, E., and Prattis, D. 2001. Kinetic study of the thermal decomposition of calcium carbonate by isothermal methods of analysis. *European Journal of Mineral Processing and Environmental Protection,* vol. 1, no.2. p. 89–102.

Hamuyuni, J., Saarenmaa, J., Mäkelä, P. Pekkala, O., Binder, C., Rannantie, S., and Lindgren, M. 2021. Pretreatment of Manganese Ore for Improved Energy Efficiency and Smelting Furnace Stability. *SSRN Electronic Journal [Preprint]*. doi.org/10.2139/ssrn.3926120

Hills, A.W.D. 1968. The mechanism of the thermal decomposition of calcium carbonate. *Chemical Engineering Science*, vol. 23, no. 4. pp. 297–320. doi.org/10.1016/0009-2509(68)87002-2

Hockaday, L., Reynolds, Q.G., Dinter, F., and Harms, T. 2018. Solar thermal treatment of manganese ores. *AIP Conference Proceedings, SolarPACES 2017: International Conference on Concentrating Solar Power and Chemical Energy Systems*, Santiago, Chile: AIP Publishing. p. 140001. doi.org/10.1063/1.5067152

Hockaday, L., Dinter, F., Harms, T., and Reynolds, Q. 2019. The solar thermal treatment of manganese ore pellets using closed-loop forced convection of air. *SOLARPACES 2018: International Conference on Concentrating Solar Power and Chemical Energy Systems*, Casablanca, Morocco, p. 150003. doi.org/10.1063/1.5117659

Hockaday, L., McKechnie, T., von Puttkamer, M.N., and Lubkpol, M. 2020. The Impact of Solar Resource Characteristics on Solar Thermal Pre-heating of Manganese Ores. *Energy Technology 2020: Recycling, Carbon Dioxide Management, and Other Technologies*. Chen, X., Zhong, Y., Zhang, L., Howarter, J.A., Baba, A.A., Wang, C., Sun, Z., Zhang, M., Olivetti, E., Luo, A., and Powell, A. (eds). Springer Cham. pp. 3–13. doi.org/10.1007/978-3-030-36830-2_1

Hockaday, L., Reynolds, Q., McGrgor, C., and Dinter, F. 2021. A Comparison of Direct Concentrating Solar Thermal Treatment of Manganese Ores to Fossil Fuel Based Thermal Treatments. *SSRN Electronic Journal [Preprint]*. doi.org/10.2139/ssrn.3926254

Hockaday, L. 2023. Solar Thermal Treatment of Manganese Ores. PhD thesis, University of Stellenbosch. http://hdl.handle.net/10019.1/127034

Ishak, R. and Tangstad, M. 2007. Degree of prereduction without coke consumption in industrial furnaces. *Proceedings of INFACON XI*, New Delhi, India: Indian Ferro Alloy Producers' Association. pp. 268–279. https://www.pyrometallurgy.co.za/InfaconXI/ (accessed: 16 November 2020)

Julia, N., Hecquet, A., Nussbaum, G., Blancher, S., and Amalric, A. 2021. Pre-Heating Manganese Ore in a Pilot-Scale Rotary Kiln. *SSRN Electronic Journal [Preprint]*. doi.org/10.2139/ssrn.3926242

Kazdal, T., Richter, S., Lang, S., inder, C., and Reuter, M. 2021. Process Design for the Pre-Treatment of Manganese Ores. *SSRN Electronic Journal [Preprint]*. doi.org/10.2139/ssrn.3926619

Mckechnie, T., McGregor, C., and Venter, G. 2020. Concentrating Solar Thermal Process Heat for Manganese Ferroalloy Production: Plant Modelling and Thermal Energy Storage Dispatch Optimization. *ASME 2020 Proceedings of the 14th International Conference on Energy Sustainability*. American Society of Mechanical Engineers. p. V001T14A001. doi.org/10.1115/ES2020-1635

Olsen, S.E., Tangstad, M., and Lindstad, T. 2007. *Production of manganese ferroalloys*. Tapir Academic Press.Trondheim, Norway.

Outotec. 2019. HSC Chemistry. https://www.outotec.com/products/digital-solutions/hsc-chemistry/ (accessed: 18 May 2019)

Pienaar, P.C. and Smith, F.P. 1992. A Case Study of the Production of High-grade Manganese Sinter from Low-grade Mamatwan Manganese Ore. *INFACON 6, Proceedings of the 6th International Ferroalloys Congress*, Cape Town. *Proceedings of the 6th International Ferroalloys Congress*, Cape Town. *South African Institute of Mining and Metallurgy,* Johannesburg. pp. 131–138. https://pyrometallurgy.co.za/InfaconVI/1131-Pienaar.pdf

Roine, A. and Bjorklund, P. 2002. Outokumpu HSC Chemistry for Windows. 02103-ORC-T. Outotec Research Oy, Finland

Serov, G.V. 2007. 'Thermal preparation of carbonate-type manganese ore for smelting'. *Steel in Translation*, vol. 37, no. 7. pp. 623–629. doi.org/10.3103/S0967091207070169

Steenkamp, T.D., Maphutha, P., Makwarela, O., Banda, W.K., Thobadi, I., Sitefane, M., Gous, J., and Sutherland, J.J. 2018. Silicomanganese production at Transalloys in the twenty-tens. *Journal of the Southern African Institute of Mining and Metallurgy*, vol. 118, no. 3. pp. 309–320. doi.org/10.17159/2411-9717/2018/v118n3a13

Tanabe, I. 1968. Preheating of Ore for a Ferromanganese Furnace-A Recent Trend in Japan. *Journal of Metals*, vol. 20. pp. 81–87. doi.org/10.1007/BF03378711

Tangstad, M., Ichihara, K., and Ringdalen, E. 2015. Pretreatment Unit in Ferromanganese Production. *INFACON XIV. Proceedings of the Fourteenth International Ferroalloys Congress.* Kiev, Ukraine. pp. 99–106. https://www.pyrometallurgy.co.za/InfaconXIV/099-Tangstad.pdf (accessed: 4 October 2019).

Terayama, K. and Ikeda, M. 1983. Study on Thermal Decomposition of MnO_2 and Mn2O3 by Thermal Analysis'. *Transactions of the Japan Institute of Metals*, vol. 24, no. 11. pp. 754–758. doi.org/10.2320/matertrans1960.24.754

Zhang, B. and Xue, Z.-L. 2013. Kinetics Analyzing of Direction Reduction on Manganese Ore Pellets Containing Carbon'. *International Journal of Nonferrous Metallurgy*, vol. 02, no. 03. pp. 116–120. doi.org/10.4236/ijnm.2013.23017 ◆